

# Absolute cross-section measurements for electron-impact single ionization of $\text{Si}^{4+}$ and $\text{Si}^{5+}$

J. S. Thompson\*

*Joint Institute for Laboratory Astrophysics of the University of Colorado and the National Institute for Standards and Technology,  
Boulder, Colorado 80309-0440*

D. C. Gregory†

*Physics Division, Oak Ridge National Laboratory, Oak Ridge, Tennessee 37831-6372*

(Received 23 February 1994)

Experimental measurements of absolute cross sections are presented for electron-impact single ionization of  $\text{Si}^{4+}$  and  $\text{Si}^{5+}$ . The incident electron energies range from below threshold to 1500 eV. The measurements were performed using the crossed ion-electron beams apparatus at the Oak Ridge National Laboratory Electron-Cyclotron Resonance Ion-Source Facility. The data are in reasonable agreement with cross sections calculated using the Lotz semiempirical formula. Reduced cross sections for the isoelectronic targets,  $\text{Si}^{4+}$  and  $\text{Ar}^{8+}$ , are compared in order to test classical scaling for direct electron-impact single ionization.

PACS number(s): 34.80.Kw

## I. INTRODUCTION

Much of the research into the properties of multiply charged ions has been driven by interest in fusion, astrophysical plasmas, and other high-temperature plasmas which are strongly influenced by the collisional properties and structure of high-charge-state ions. Electron-impact ionization cross sections are important ingredients for the development of models and improved diagnostic techniques for the analysis of high-temperature plasmas. The diversity of the ion species and charge states contained in a hot plasma makes it difficult theoretically and nearly impossible experimentally to produce all the cross sections and rate coefficients necessary to model a plasma. A number of semiempirical formulas and classical scaling rules have been widely used to generate the data needed for the plasma models and to generalize the measured data to other ionized species. This paper reports the measurement of absolute cross sections for electron-impact single ionization of  $\text{Si}^{4+}$  and  $\text{Si}^{5+}$  from below threshold to 1500 eV. The experimental data are compared to a widely used semiempirical method for determining direct-ionization cross sections.

Lotz [1] has proposed a semiempirical method for calculating direct electron-impact single-ionization cross sections. For ions with charge states of 4+ and higher the formula for the cross section can be written as

$$\sigma = a \sum_{i=1}^N q_i \frac{\ln(E/P_i)}{EP_i}, \quad (1)$$

where  $E$  is the energy of the incident electron in eV,  $P_i$  is the binding energy of electrons in the  $i$ th subshell in eV,  $q_i$  is the number of equivalent electrons in the  $i$ th subshell (where  $i$  ranges from 1 to  $N$ ) and  $a$  is an empirically determined constant equal to  $4.5 \times 10^{-14} \text{ cm}^2 (\text{eV})^2$ . Typically, the  $2s$  and  $2p$  subshells are considered for boron-like through neonlike ions. The predictions of the Lotz formula are often within 20% of more accurate quantal calculations for direct ionization [2].

## II. EXPERIMENTAL ARRANGEMENT

The measurements reported in this paper were performed at the Oak Ridge National Laboratory Electron-Cyclotron Resonance (ORNL-ECR) Ion-Source Facility, using a crossed electron-ion beams apparatus. This apparatus has been described in detail in previous papers [3,4], therefore only a brief discussion will be given here.

Multiply charged ions of silicon are created by introducing silane ( $\text{SiH}_4$ ) into the ECR region of the ion source. The ion beam is transported to the high-vacuum chamber shown in Fig. 1 through a beam line containing ion optics and differential pumping. The pressure in the chamber was typically  $5 \times 10^{-7} \text{ Pa}$  under experimental conditions. After entering the chamber, the ion beam can be steered and focused using one-dimensional Einzel lenses. A parallel plate electrostatic analyzer (labeled charge purifier in the figure) is used to remove from the beam ions that have changed charge due to collisions with background gas or grazing collisions with slits or apertures. The ions then pass through the collision region, where they intersect an electron beam at  $90^\circ$ . After passing through the collision region, the charge states of the beam are separated by a double-focusing magnetic

\*Present address: Department of Physics, University of Nevada, Reno, NV 89557.

†Present address: Office of Radiation Protection, Oak Ridge National Laboratory, Bldg. 5505, MS-6375, Oak Ridge, TN 37831-6375.

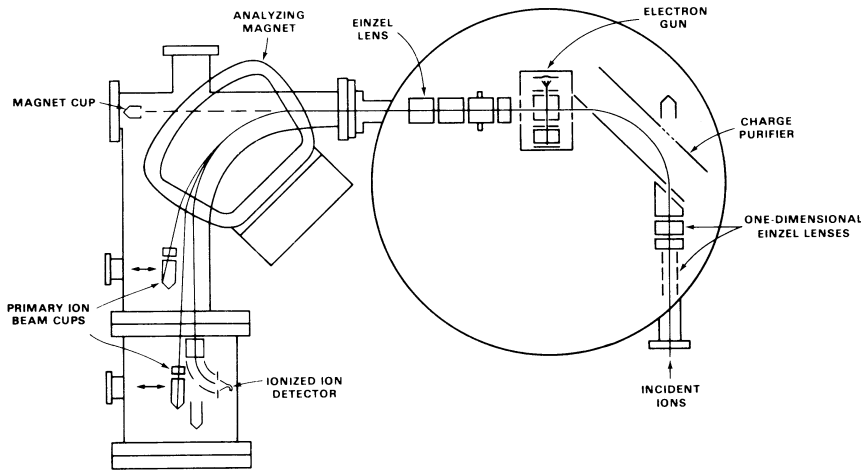


FIG. 1. Schematic of crossed-beams collision chamber and postcollision magnetic analyzer. See text for details.

sector analyzer. The signal ions, with the same velocity as the incident beam, but a higher charge state, are focused onto the channel-electron-multiplier labeled "ionized ion detector" in the figure. The signal ions are deflected through  $90^\circ$ , out of the scattering plane, by an electrostatic cylindrical-sector analyzer before detection in order to reduce the background counts caused by stray particles and photons. The detection efficiency for the signal ions is near 100% [5], and the sensitivity of the electronics is monitored by periodic pulse-height distribution measurements. Ions that traverse the collision region without being ionized are collected in one of two movable Faraday cups, depending on the incident-to-signal ion charge ratio. Additional lenses and Faraday cups shown in the ion-beam path are used for beam tuning and diagnostic tests to ensure complete collection of the signal ions. The absolute ion-beam current and accelerating voltage are carefully monitored.

The electron gun used in the experiments is a modified version of the one described by Taylor *et al.* [6]. The electron beam is confined by a 250-G axial magnetic field which enhances the uniformity of the beam density and reduces the physical size of the electron beam in the collision volume over a wide range of electron velocities. The electron and ion beams cross at  $90^\circ$ . The electron beam is collected and monitored on an edge-on array of tantalum "razor blades" designed to minimize back-scattering and secondary electron emission. The electron velocity in the collision region is derived from the accelerating voltage, including corrections for contact potentials and the beam space charge based on previous calibrations [3,5]. Uncertainties in the quoted collision energy range from  $\pm 0.2$  eV at the lower energies to  $\pm 1$  eV at 1500 eV. The energy spread in the electron beam is estimated to be between 1 and 2.5 eV over this energy range [3].

The absolute cross section  $\sigma$  for electron-impact ionization at the collision energy  $E$ , where the electron and ion beams cross at  $90^\circ$ , is given by the expression

$$\sigma(E) = \frac{Rqe^2v_i v_e F}{I_i I_e (v_i^2 + v_e^2)^{1/2} D} \quad (2)$$

Here  $R$  is the signal count rate,  $e$  is the electron charge,  $qe$  is the charge of the incident ions,  $v_i$  and  $v_e$  are ion and electron velocities,  $I_i$  and  $I_e$  are the ion- and electron-beam currents,  $D$  is the detection efficiency of a signal event, and  $F$  is the form factor. The form factor, a measure of the spatial overlap of the two beams, is determined by sweeping a probe with a narrow slit through each beam. The transmitted current is detected as a function of slit position and the form factor is calculated from the overlap of the beam profiles.

The uncertainties listed in the data tables and plotted on the graphs are reported at the equivalent of two standard deviations for statistical uncertainties, relative only, and at the 90% confidence level for absolute uncertainties. Relative uncertainties were dominated by counting statistics, but also include other factors, such as form-factor values, which differ slightly between measurements due to changes in the ion beam. The relative contributions dominate the absolute uncertainties, but other contributing factors include the transmission and detection efficiency of the signal ions, current measurements, and particle velocities. Details of the error analysis have been reported in previous publications [7,8]. Absolute uncertainties at the 90% confidence level were obtained from the quadrature sum of twice the quoted relative uncertainties and 7% from the other measured quantities in Eq. (2). The absolute uncertainties for these measurements range from 7 to 10 % for typical points near the peak of the cross-section curve at a 90% confidence level (equivalent to two standard deviations for statistical uncertainties).

### III. RESULTS

The electron-impact single-ionization cross-section measurements are listed in Tables I and II and plotted in Figs. 2 and 3 for  $\text{Si}^{4+}$  and  $\text{Si}^{5+}$ , respectively. Cross sections measured at the same incident electron energy were combined using a variance-weighted unbiased mean for cross sections that had overlapping error bars.

In these experiments, a double-focusing magnetic sector analyzer dispersed the ions extracted from the ion

source and was used to select the ion beam for transmission to the experimental chamber. A magnetic analyzer disperses the ions according to their mass-to-charge ratio ( $m/q$ ). In the case of the  $\text{Si}^{4+}$  experiment, the ion beam could contain a component consisting of the impurity ion  $^{14}\text{N}^{2+}$ . Cross sections were measured for the isotopes  $^{28}\text{Si}^{4+}$  and  $^{29}\text{Si}^{4+}$  at incident electron energies of either 385 or 483 eV for every data set. The purity of the beam could then be determined since the mass-to-charge ratio for  $^{29}\text{Si}^{4+}$  is unique. The  $^{28}\text{Si}^{4+}$  ion beam was found to be at least 99% pure for each data set. The natural occurring abundance of  $^{29}\text{Si}^{4+}$  is only 4.67% [9], which made measuring the  $^{29}\text{Si}^{4+}$  cross-section data impractical over the entire range of incident electron energies.

The cross-section data for the electron-impact single ionization of  $\text{Si}^{4+}$  are shown plotted in Fig. 2 along with absolute uncertainties at the 90% confidence level, where

TABLE I. Experimental electron-impact single-ionization cross sections for  $\text{Si}^{4+}$ . Relative uncertainties listed are two standard deviations. The absolute uncertainties at a 90% confidence level are listed in parentheses.

Electron energy (eV)	Cross section ( $10^{-18} \text{ cm}^2$ )
33.4	$-0.002 \pm 0.044$ (0.044)
46.5	$0.043 \pm 0.028$ (0.028)
48.4	$0.034 \pm 0.040$ (0.040)
60.8	$0.043 \pm 0.036$ (0.036)
72.4	$0.151 \pm 0.030$ (0.032)
84.6	$0.240 \pm 0.026$ (0.031)
96.0	$0.276 \pm 0.026$ (0.032)
97.4	$0.282 \pm 0.028$ (0.034)
121	$0.474 \pm 0.028$ (0.044)
146	$0.681 \pm 0.032$ (0.057)
169	$0.847 \pm 0.030$ (0.067)
181	$1.344 \pm 0.022$ (0.098)
194	$1.892 \pm 0.022$ (0.136)
206	$2.289 \pm 0.024$ (0.163)
218	$2.634 \pm 0.034$ (0.190)
242	$3.242 \pm 0.028$ (0.231)
266	$3.718 \pm 0.028$ (0.264)
290	$4.043 \pm 0.024$ (0.287)
337	$4.491 \pm 0.026$ (0.319)
385	$4.62 \pm 0.16$ (0.36)
434	$4.929 \pm 0.042$ (0.351)
483	$5.081 \pm 0.034$ (0.361)
532	$5.270 \pm 0.050$ (0.376)
581	$5.349 \pm 0.102$ (0.392)
639	$5.316 \pm 0.016$ (0.376)
688	$5.07 \pm 0.30$ (0.47)
738	$5.01 \pm 0.04$ (0.36)
788	$4.82 \pm 0.06$ (0.35)
836	$4.78 \pm 0.04$ (0.34)
886	$4.77 \pm 0.02$ (0.34)
936	$4.68 \pm 0.04$ (0.33)
986	$4.85 \pm 0.16$ (0.38)
1085	$4.62 \pm 0.04$ (0.33)
1181	$4.52 \pm 0.10$ (0.33)
1330	$4.62 \pm 0.20$ (0.38)
1487	$4.14 \pm 0.14$ (0.32)

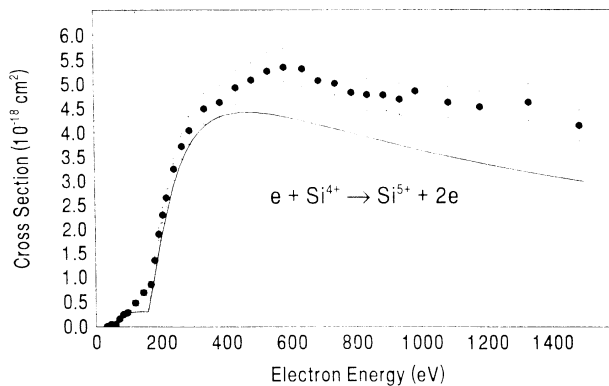


FIG. 2. Absolute cross sections for electron-impact single ionization of  $\text{Si}^{4+}$  as a function of incident electron energy. The solid circles represent the measured cross sections. The error bars represent absolute uncertainties at the 90% confidence level. The solid line represents the Lotz cross section with 5% of the ion beam in the  $(1s^2 2s^2 2p^5 3s)$  metastable state. The dot-dashed line is the Lotz cross-section times 1.17.

TABLE II. Experimental electron-impact single-ionization cross sections for  $\text{Si}^{5+}$ . Relative uncertainties listed are two standard deviations. The absolute uncertainties (listed in parentheses) are reported at a 90% confidence level.

Electron energy (eV)	Cross section ( $10^{-18} \text{ cm}^2$ )
196	$0.010 \pm 0.060$ (0.060)
208	$0.093 \pm 0.044$ (0.044)
220	$0.510 \pm 0.052$ (0.063)
231	$0.841 \pm 0.036$ (0.070)
243	$1.108 \pm 0.040$ (0.088)
268	$1.483 \pm 0.038$ (0.112)
293	$1.816 \pm 0.028$ (0.131)
317	$2.042 \pm 0.034$ (0.148)
341	$2.288 \pm 0.032$ (0.165)
365	$2.421 \pm 0.038$ (0.175)
390	$2.566 \pm 0.030$ (0.184)
415	$2.687 \pm 0.036$ (0.193)
440	$2.804 \pm 0.042$ (0.202)
463	$2.861 \pm 0.024$ (0.204)
487	$2.95 \pm 0.16$ (0.26)
537	$3.136 \pm 0.040$ (0.225)
588	$3.03 \pm 0.22$ (0.31)
635	$3.136 \pm 0.030$ (0.224)
683	$3.121 \pm 0.034$ (0.223)
733	$3.069 \pm 0.020$ (0.218)
783	$3.036 \pm 0.016$ (0.215)
831	$3.068 \pm 0.026$ (0.218)
887	$2.879 \pm 0.036$ (0.207)
936	$2.870 \pm 0.028$ (0.205)
987	$2.804 \pm 0.036$ (0.202)
1085	$2.726 \pm 0.036$ (0.196)
1185	$2.69 \pm 0.22$ (0.291)
1284	$2.515 \pm 0.030$ (0.180)
1382	$2.56 \pm 0.13$ (0.22)
1481	$2.52 \pm 0.10$ (0.20)

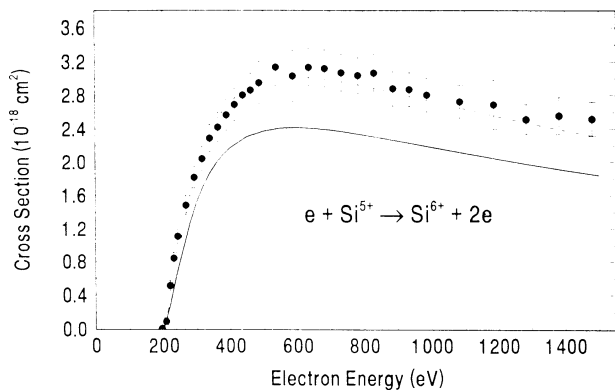


FIG. 3. Absolute cross sections for electron-impact single ionization of  $\text{Si}^{5+}$  as a function of incident electron energy. The solid circles represent the measured cross sections. The error bars represent absolute uncertainties at the 90% confidence level. The solid line represents the Lotz cross section. The dot-dashed line is the Lotz cross-section times 1.25.

they are larger than the plotted points. The incident electron energy ranges from below threshold to 1500 eV. The ground-state ( $1s^2 2s^2 2p^6$ ) ionization threshold was determined to be 166.4 eV using the relativistic Hartree-Fock (HFR) code developed by Cowan [10]. The cross section is nonzero below the ground-state ionization threshold indicating that the ion beam contains a metastable component. The  $\text{Si}^{4+}$  ion has a long-lived metastable configuration ( $1s^2 2s^2 2p^5 3s$ ) with a threshold energy of 52.6 eV for electron-impact single ionization of the 3s electron [10]. This metastable state is assumed to be responsible for the nonzero cross-section measurements below the ionization threshold energy of the  $\text{Si}^{4+}$  ground state due to the observed onset near 50 eV.

The metastable fraction of the  $\text{Si}^{4+}$  beam is determined by comparing the Lotz prediction for the direct ionization of the 3s electron from the metastable state with the measured cross section near the 52.6 eV threshold. Assuming a metastable beam component of 5%,  $\text{Si}^{4+}(1s^2 2s^2 2p^5 3s)$  gives a very good agreement with the measured cross-section data between 50 and 100 eV. The solid line in the figure is the cross section predicted by the Lotz formula assuming that the ion beam consists of 95% of the ions in the ( $1s^2 2s^2 2p^6$ ) ground state and 5% of the ions in the ( $1s^2 2s^2 2p^5 3s$ ) metastable state. The Lotz cross section underestimates the magnitude of the measured cross section by about 17%, but is in general agreement with the qualitative characteristics of the data. A closer examination, however, shows that there are significant discrepancies in the threshold and high-energy regions, which warrant further discussion. More elaborate calculations for comparison with the data have not been published.

The discrepancy between the Lotz cross section and the measured data below the ground-state threshold for  $\text{Si}^{4+}$  (between 100 and 150 eV) can be attributed to contributions to the cross section from inner-shell excitation followed by autoionization. Pindzola, Griffin, and

Bottcher [11] have performed calculations that show excitation-autoionization processes can greatly enhance the electron-impact ionization cross section for neonlike ions in the metastable  $2p^5 3s$  configuration. The indirect cross section is dominated by  $2p^5 3s \rightarrow 2p^4 3s 3l$  excitations. Recent electron-impact ionization cross-section measurements [12] for  $\text{Ar}^{8+}$  have shown that the excitation-autoionization contribution to the  $2p^5 3s$  metastable state cross section, below the ground-state threshold, is approximately five times the direct cross section. The excitation energies for the  $2p \rightarrow 3l$  transitions in  $\text{Si}^{4+}$  were calculated using Cowan's HFR code [10]. The excitation energies are 121.9, 130.6, and 144.9 eV for the  $2p \rightarrow 3s$ ,  $3p$ , and  $3d$  transitions, respectively. The excitation energies agree with the onset of the observed rise in the data above the Lotz cross section for the metastable component of the  $\text{Si}^{4+}$  beam at electron-impact energies above 121 eV. The observed enhancement of the electron-impact ionization cross section for the  $2p^5 3s$  configuration of  $\text{Si}^{4+}$  between 100 and 150 eV is approximately three times the cross section for direct ionization processes as predicted by Lotz's method in this energy range.

Above 1000 eV the measured cross-section data do not follow the shape of the Lotz prediction. Contributions from inner-shell excitation followed by autoionization for electron-impact ionization of the ground state of  $\text{Si}^{4+}$  are considered to be negligible [11] in this energy range. A systematic error in the cross-section measurements at high energies may be the cause of the deviation of the data. The heating of the electron-beam collector caused by the higher energy electron beams can lead to a local increase in the pressure near the collector. The increase in pressure results in electron scattering from residual gas atoms and molecules and decreases the electron current monitored at the collector. The scattering of the electron beam occurs near the interaction region and can effectively increase the apparent cross section. This effect was not observed in the  $\text{Si}^{5+}$  measurements, indicating that the electron-beam collector was sufficiently outgassed for those measurements.

Data for the electron-impact single-ionization cross sections for  $\text{Si}^{5+}$  are shown graphically in Fig. 3. Absolute uncertainties are shown at the 90% confidence level except where smaller than the data points. In the ion-source plasma, the mass-to-charge ratio for  $^{28}\text{Si}^{5+}$  was unique, so the ion beam was pure. Cross-section data are shown for incident electron energies ranging from below the ( $1s^2 2s^2 2p^5$ ) ground-state threshold [10] at 207.7 eV to 1500 eV. No evidence for contributions to the cross section from metastable components in the beam was observed in the cross-section data. The solid line in the figure is the cross section predicted by the Lotz formula. Comparison of the Lotz cross section with the measurements indicates that direct ionization dominates the total ionization cross section over the range of reported electron energies. Detailed calculations for comparison with the  $\text{Si}^{5+}$  cross-section data do not presently exist.

Cross sections of isoelectronic ions for direct electron-impact ionization can be compared using a scaling relationship taken from a classical theory for Coulomb

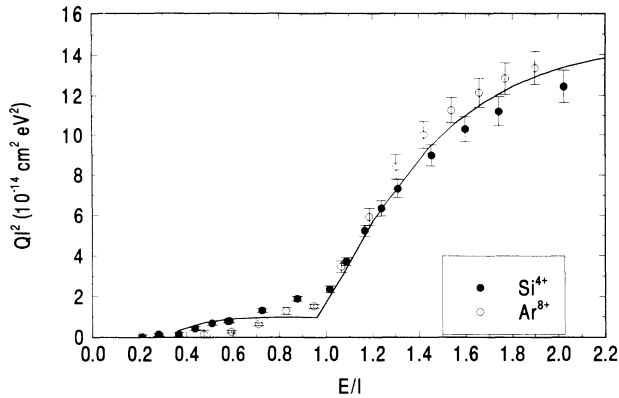


FIG. 4. Reduced cross sections  $I^2Q$  vs incident electron energy in  $2p$  threshold energy units  $E/I$ . The solid circles represent the  $\text{Si}^{4+}$  data. The open circles are the reduced data for  $\text{Ar}^{8+}$  (from Ref. [12]). The error bars represent absolute uncertainties at the 90% confidence level for the cross-section measurements. The solid line represents the reduced Lotz cross section (multiplied by 1.17) with 5% of the ion beam in the  $(1s^22s^22p^33s)$  metastable state.

scattering of two electrons as derived by Thomson [13]. The cross section for direct ionization  $Q$  may be represented in terms of the ionization potential  $I$  as a function of the incident electron energy in threshold units  $E/I$  by the equation

$$I^2Q = f(E/I). \quad (3)$$

The complete formula should contain a dependence on the atomic number  $Z$ , based on quantum-mechanical considerations [14–17]. However, the above formula is useful for comparing and estimating ionization cross sections for isoelectronic systems.

The reduced cross sections  $I^2Q$  for  $\text{Si}^{4+}$  are plotted in Fig. 4 as a function of electron energy in  $2p$  ionization

threshold units. They are compared to the reduced data for the isoelectronic  $\text{Ar}^{8+}$  ion, which was measured by Zhang *et al.* [12]. The reduced data are in good agreement in the energy region from threshold to twice the ionization energy. Both sets of reduced data also exhibit the characteristic nonzero cross section below the ground-state ionization energy, which indicates the presence of metastable ions in the beams.

#### IV. CONCLUSIONS

Absolute cross sections for electron-impact single ionization of  $\text{Si}^{4+}$  and  $\text{Si}^{5+}$  are reported. The incident electron energy ranges from below threshold to 1500 eV. The shape of the measured cross-section curves agree with the semiempirical Lotz cross section for direct ionization, but the magnitudes of the measured cross sections are approximately 20% greater than the predictions of the Lotz formula. The  $\text{Si}^{4+}$  cross-section data exhibit evidence for a metastable component in the ion beam, but no evidence for significant distinct indirect-ionization features were observed in the cross-section data for electron-impact ionization of the ground state for either charge state of the silicon ion. The cross-section data for the metastable component of the  $\text{Si}^{4+}$  beam exhibits evidence of contributions to the total cross section from indirect processes. The reduced cross sections for  $\text{Si}^{4+}$  and isoelectronic  $\text{Ar}^{8+}$  targets were shown to be in good agreement from below the ground-state threshold to twice the  $2p$  ionization limit.

#### ACKNOWLEDGMENTS

The authors acknowledge the expert technical advice and assistance of J. W. Hale in the operation of the ion source. This work was supported by the Office of Fusion Energy, U.S. Department of Energy, under Contract No. DE-A105-86ER53237 with the National Institute of Standards and Technology and Contract No. DE-AC05-84OR21400 with Martin Marietta Energy Systems, Inc.

- [1] W. Lotz, *Z. Phys.* **206**, 205 (1967); **216**, 241 (1968); **220**, 466 (1969).
- [2] G. H. Dunn, *Nucl. Fusion* **2**, 25 (1992).
- [3] D. C. Gregory, L. J. Wang, F. W. Meyer, and K. Rinn, *Phys. Rev. A* **35**, 3256 (1987).
- [4] F. W. Meyer, *Nucl. Instrum. Methods Phys. Res. Sect. B* **9**, 532 (1985).
- [5] D. C. Gregory, M. S. Huq, F. W. Meyer, D. R. Swenson, M. Sataka, and S. Chantrenne, *Phys. Rev. A* **41**, 106 (1990).
- [6] P. O. Taylor, K. T. Dolder, W. E. Kauppila, and G. H. Dunn, *Rev. Sci. Instrum.* **45**, 538 (1974).
- [7] D. H. Crandall, R. A. Phaneuf, and P. O. Taylor, *Phys. Rev. A* **18**, 1911 (1978).
- [8] D. C. Gregory, F. W. Meyer, A. Müller, and P. Defrance, *Phys. Rev. A* **34**, 3657 (1986).
- [9] *Handbook of Chemistry and Physics*, 72nd ed. (CRC, Boca Raton, FL, 1992).
- [10] R. D. Cowan, *The Theory of Atomic Structure and Spectra* (University of California Press, Berkeley, 1981); R. D. Cowan and D. C. Griffin, *J. Opt. Soc. Am.* **66**, 1010 (1976).
- [11] M. S. Pindzola, D. C. Griffin, and C. Bottcher, *Phys. Rev. A* **41**, 1375 (1990).
- [12] Y. Zhang, C. B. Reddy, R. S. Smith, D. E. Golden, D. W. Mueller, and D. C. Gregory, *Phys. Rev. A* **44**, 4368 (1991).
- [13] J. J. Thomson, *Philos. Mag.* **23**, 449 (1912); *Physics of Ion Impact Phenomena*, edited by Deepak Mathur (Springer-Verlag, Berlin, 1991), pp. 13–86.
- [14] E. J. McGuire, *Phys. Rev. A* **16**, 73 (1977).
- [15] D. L. Moores, L. B. Golden, and D. H. Sampson, *J. Phys. B* **13**, 385 (1980).
- [16] S. M. Younger, *Phys. Rev. A* **24**, 1278 (1981).
- [17] S. M. Younger, *Phys. Rev. A* **25**, 3396 (1982).